This is a repository copy of *Retrofit Design Methodology for Substandard R.C. Buildings with Torsional Sensitivity*.

White Rose Research Online URL for this paper:
https://eprints.whiterose.ac.uk/115226/

Version: Accepted Version

Article:
Thermou, G.E. orcid.org/0000-0002-9569-0176 and Psaltakis, M. (2018) Retrofit Design Methodology for Substandard R.C. Buildings with Torsional Sensitivity. Journal of Earthquake Engineering, 22 (7). pp. 1233-1258. ISSN 1363-2469

https://doi.org/10.1080/13632469.2016.1277569

Reuse
Items deposited in White Rose Research Online are protected by copyright, with all rights reserved unless indicated otherwise. They may be downloaded and/or printed for private study, or other acts as permitted by national copyright laws. The publisher or other rights holders may allow further reproduction and re-use of the full text version. This is indicated by the licence information on the White Rose Research Online record for the item.

Takedown
If you consider content in White Rose Research Online to be in breach of UK law, please notify us by emailing eprints@whiterose.ac.uk including the URL of the record and the reason for the withdrawal request.

eprints@whiterose.ac.uk
https://eprints.whiterose.ac.uk/

Retrofit design methodology for substandard R.C. buildings with torsional sensitivity

Georgia E. Thermou[‡1, 2] and Manousos Psaltakis[3§]

[1] Department of Civil Engineering, Aristotle University of Thessaloniki, 54124, Thessaloniki, Greece (on leave)

[2] Civil and Structural Engineering Department, The University of Sheffield, S1 3JD, Sheffield, UK

[3] Department of Civil and Environmental Engineering, Imperial College, SW7 2AZ, London, UK

Recent earthquakes have revealed the susceptibility of non-ductile reinforced concrete (R.C.) buildings with deficiencies related to stiffness and/or mass irregularities in plan and elevation. This paper proposes a design methodology for the seismic upgrading of rotationally sensitive substandard R.C. buildings. The methodology aims first to eliminate the effect of torsional coupling on modal periods and shapes and then modify the lateral response shape of the building in each direction so as to achieve an optimum distribution of interstorey drift along the building height. A case study is used to illustrate practical application of the proposed methodology.

Keywords: Assessment; Retrofitting; Torsion; Buildings; Reinforced Concrete; Displacement-based design

---

[‡] Corresponding author, Assistant Professor, E-mail: gthermou@civil.auth,gr

[§] MSc student, Civil Engineer, E-mail: manousoscivil@hotmail.gr

1. Introduction

The majority of multi-storey R.C. buildings in southern Europe were built in the first half of the 20th century. Most of the structures were designed for gravity loads only by implementing the allowable stress design philosophy which did not allow any control of the mode of failure and the corresponding deformation capacity of the individual members. The first seismic codes were introduced in 1960s with seismic detailing being at a primitive stage of knowledge. The fact that the modern seismic codes were introduced much later (more than 20 years later), in the mid-1980s, constitutes a rather alarming issue considering the decreased level of seismic protection and the increased seismic vulnerability of the vast majority of the built environment. Strong earthquake events have repeatedly illustrated the deficiencies of non-ductile R.C. buildings at member- and/or system-level. Insufficient reinforcement detailing of components limit the ability of the whole structure to resist seismic loading since deformation demands are such that exceed the available deformation capacity of the structure and thus the vertical load bearing capacity (i.e., the structure can no longer support its self-weight and collapses). System-level deficiencies such as eccentricities of stiffness and mass in both plan and elevation are common in existing structures leading to severe damage and eventually to collapse. In-height irregularities may result due to the practice of setbacks or penthouses in the upper floors. A special case of in-height irregularities is the soft-storey formation in pilotis type buildings which are common in southern Europe (i.e., the ground storey used for commercial facilities is an open frame (bare frame), while the storeys above are infilled). In-plan irregularities may result due to the uneven distribution of stiffness in plan (horizontal irregularities) as a result of architectural (e.g., L-shaped buildings or skew-plans) or functional (e.g., facade of commercial buildings) features. Moreover, the position of the elevator shaft walls plays an important role in the distribution of stiffness in plan.

The reduction of seismic risk through assessment and rehabilitation programs to upgrade buildings that are deemed inadequate with regards the level of seismic protection they provide to the public has become

a recognized priority. Different retrofit strategies may be developed for non-ductile R.C. buildings depending among other parameters on: (a) the mandated level of the intervention; (b) the level of knowledge about materials, geometry and detailing; (c) hazard parameters, including the definition of appropriate ground motion levels and their probability to occur; and (c) the financial objectives of the retrofit effort [Thermou and Elnashai, 2006; Calvi, 2013; Zerbin and Aprile, 2015; Mazza, 2015]. Among others, Thermou et al. [2007, 2012a, b] developed a retrofit design concept according to which response may be improved by targeting for a fundamental mode shape that would produce a desirable pattern of interstorey drift and therefore damage. This concept was further extended by Pardalopoulos and Pantazopoulou [2011] in three-dimensional structures with torsional component in their lateral response, where in the methodology developed the fundamental translational mode shape is approximated by separating the contributions to translation and twisting from the corresponding basic modes of an associated decoupled system.

Distribution rather than localization of damage is crucial; otherwise the weakest link will jeopardize the stability of the whole structure [Thermou et al., 2007, 2012a, b]. In the proposed retrofit design methodology, the general criteria that need be satisfied are correction of any irregularities in plan and in elevation and elimination of mechanisms likely to lead to damage localization. Another important issue is the modification of the structural system so as to increase the redundancy of the lateral load resisting system.

This paper presents a design methodology for the seismic upgrading of rotationally sensitive existing R.C. buildings. The methodology aims first to eliminate the effect of torsional coupling on modal periods and shapes. After this stage, the building is expected to respond independently in the two lateral directions (since torsional effects have been neglected) following the corresponding fundamental mode shapes. Next, the translational response shape in each orthogonal direction is engineered as to achieve an optimum distribution of interstorey drift along the building height [Thermou et al., 2007]. The proposed methodology was implemented to an existing three-storey building constructed in the early 1970s. The

validity of the proposed methodology was assessed by carrying out inelastic analyses with the use of a three-dimensional finite element model of the retrofitted structure. The results indicate the efficiency of the proposed design methodology for the seismic upgrading of existing torsionally unbalanced R.C. buildings.

2. Deficiencies of substandard R.C. buildings

The framework of modern earthquake engineering relies on regulating the distribution of stiffness and mass in order to achieve a favorable distribution of deformation demands throughout the structure, the hierarchy of failure in structures through the capacity design rules and reinforcement detailing especially in the plastic hinge regions in order to secure ductility. The presence of R.C. walls in seismic design is considered significant since global lateral drift is controlled and damage in frame elements is reduced. The introduction of walls leads to the development of dual structural systems. In such a system the support for the vertical loads is mainly provided by a spatial frame and resistance to lateral loads is contributed to in part by the frame system [EC8-Part III, 2005]. Depending on amount of the shear resistance of the walls at the building base compared to the total seismic resistance of the whole structural system, wall and wall- or frame-equivalent systems may result.

Reinforced concrete structures found in the urban areas of southern Europe built between the 1920s and 1960s were designed for gravity loads only, whereas those built between 1960s and 1980s were designed with the first generation of seismic codes. The knowledge regarding the seismic behavior of R.C. buildings back then was rather limited and design was based on lot of simplification assumptions. According to the relevant paragraphs of the first Greek Seismic Code [Royal Decree, 1959] R.C. walls should be: (i) placed in the two orthogonal directions so that the center of stiffness to be close to the center of mass and at least at the central one third of the plan and closer at the perimeter of the building; and (ii) arranged in such a way as the total area of the R.C. walls in any storey in each direction of loading to be at

least equal to 1/500 (i.e., 2‰) of the total floor plan area of the stories above. This was the basic rule of thumb used at that era. The graph in Fig. 1(a) presents the total area ratio of the R.C. walls in ground storey (first storey) and in both directions for buildings up to 8 storeys. Hence, for a well-designed 4-storey building of the 1960s the area ratio of R.C. walls in the first storey in both directions should be at least equal to 1.6%. In Fig. 1(b)–(d) some representative plan layouts of multi-storey buildings in Greece of the 1960s are shown. The lack of knowledge and experience of the average civil engineer in handling the placement of R.C. walls is evident. Nether the number of R.C. walls is sufficient according to required area ratio of walls nor the position of the wall is efficient in providing adequate torsional resistance and stiffness. This type of deficiencies are common in the building stock designed according to the first generation of seismic codes. Moreover, structures of that era are characterized by insufficient reinforcement detailing (e.g., inadequately anchored transverse and longitudinal reinforcement, sparse and smooth stirrups, lap splices in the region of the plastic hinge, no stirrups in the beam-column joints, bad connection of the ground floor columns to the foundation system), poor quality of materials, non-uniform distribution of stiffness and/or mass in plan and elevation, insufficient foundation system, and various other weaknesses such as increased loading due to change of use and corrosion of reinforcement. Taking as example the country of Greece, common features of the buildings of that era based on the standards of the period were as follows:

- Materials: Concrete grade, B120 ÷ B160 corresponding to contemporary concrete characteristic cylinder strengths 8-10 MPa; Steel grade, StI (f_{sy}=220 MPa) for both longitudinal and transverse reinforcement and StIII (f_{sy}=420 MPa) for longitudinal reinforcement as per DIN 1045 [1936].
- Column detailing: cross section dimensions 250 ÷ 600 mm, diameters of column longitudinal reinforcement Ø14 ÷ Ø20, transverse reinforcement Ø6/250 ÷ 300 mm, diameter Ø8 was rarely applied, longitudinal reinforcement ratio 7‰ ÷ 9‰ < 10‰.
- Beam detailing: cross section dimensions 100×300 ÷ 300×600 mm, diameters of beam longitudinal reinforcement bars Ø10 ÷ Ø18, beam transverse reinforcement Ø6/200 ÷ 250 mm.

- Wall detailing: thickness 150 ÷ 200 mm, length: 1.5~3.5m, boundary elements: length 200 mm, 4Ø12, web reinforcement: #Ø8/250.
- Anchorage / lap splices construction practice: longitudinal reinforcement with hooks with arbitrary lengths, stirrups anchored with 90° hooks, unconfined lap splices (Fig. 2(a)).
- Lack of a continuous vertical load path along the height of the building.
- There is no typical floor since the dimensions of the columns and beams change from storey to storey. Often in-plan column layout does not follow a grid pattern, hence leading to indirect supports (Fig. 2(b)).
- Beam-column joints were usually left without stirrups, for convenience of construction. Another commonly reported location of failure is in the beam-column joints, particularly in connections over the perimeter of an R.C. frame building.
- Foundation usually comprised single column conical-shaped, lightly reinforced footings. In well-attended structures, a network of lightly reinforced, rectangular section (200 mm by 400 mm to 500 mm) connecting beams were used to join the upper sections of all footings.

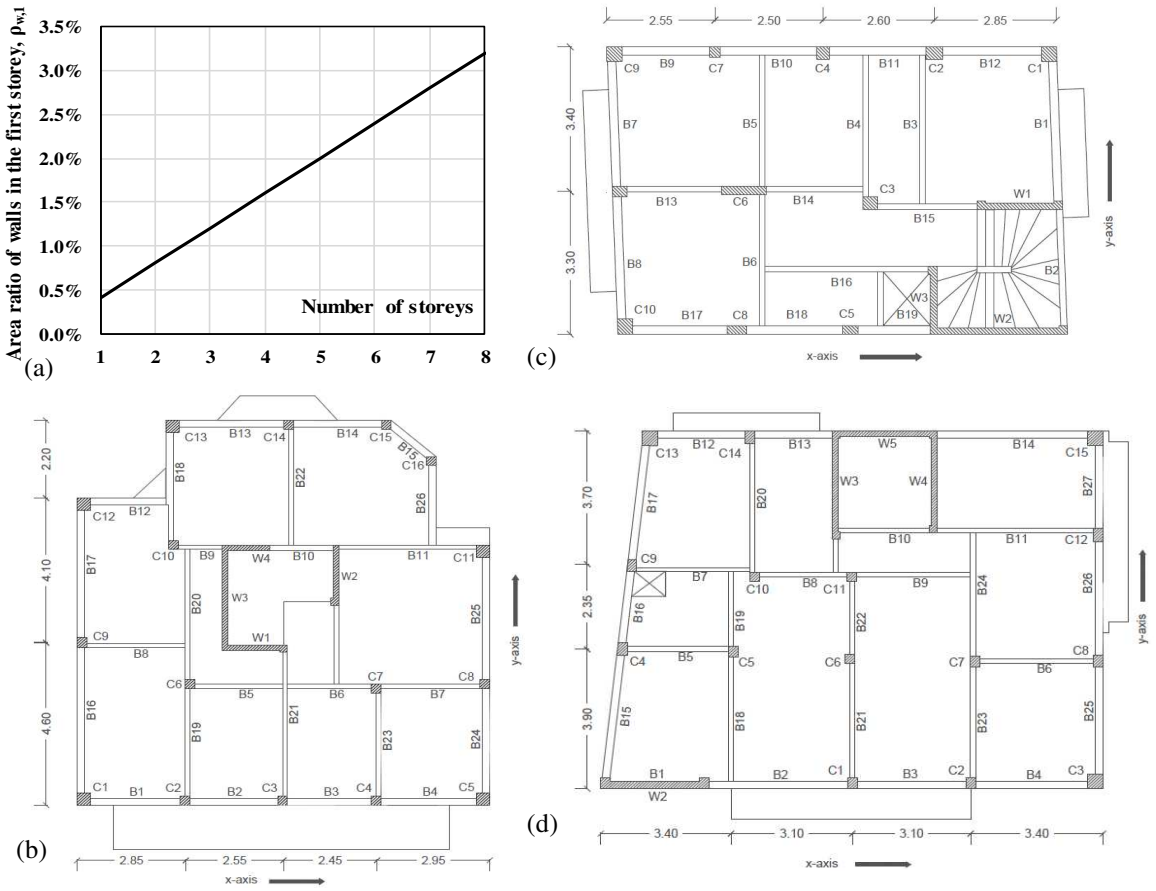

FIGURE 1 (a) Area ratio of walls in the first storey, $\rho_{w,1}$, according to the Greek Seismic Code [Royal Decree, 1959]; (b)-(d) Representative floor plan layouts of multi-storey buildings in Greece of the 1960s.

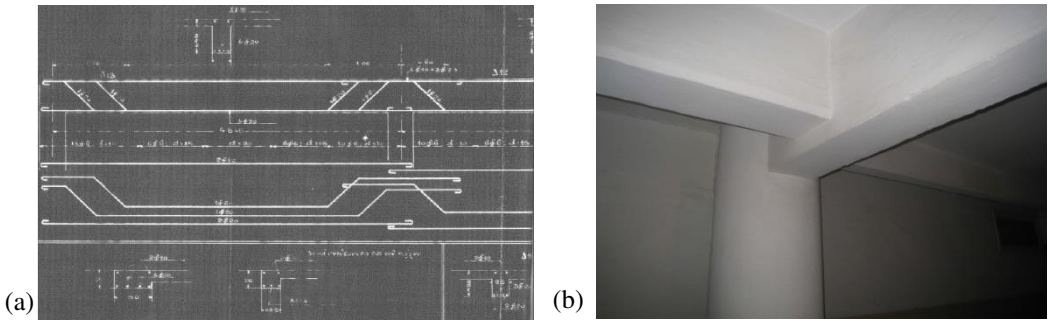

FIGURE 2 (a) Beam reinforcement detailing of the 1920s in Greece (original drawing); (b) Indirect support.

3. Proposed retrofit design methodology

The proposed retrofit design methodology aims to modify radically the response of old substandard R.C. buildings with torsional sensitivity. For this scope a retrofit design methodology has been developed which comprises two design stages. First, structural eccentricities are minimized and simultaneously torsional resistance and stiffness are enhanced. This is realized by the addition of stiffness at the periphery of the building through adoption of global intervention methods (e.g., R.C. infill walls). At the end of this design stage, the building is symmetric in plan and torsionally balanced. Thus, the ground motion in the two orthogonal axes (x-x and y-y) will cause only lateral motion, whereas the system will experience no torsional motion unless the base motion includes rotation about the vertical axis. The building is modified further as to respond in each lateral direction according to a target response shape, called hereafter target response shape. The objective is to mitigate damage localization through controlled modification of the lateral response shape. This is achieved by a weighted distribution of additional stiffness along the height of the building.

3.1 Conceptual framework

The unsymmetric plan depicted in Fig. 3(a) corresponds to the constant floor plan of an existing multistorey R.C. building. Due to the distance between the center of mass (CM) and the center of stiffness (CS) (i.e., eccentricities e_x and e_y in Fig. 3(a)), the building is expected to simultaneously undergo lateral motion in the two orthogonal directions (x-x and y-y) and torsion about the vertical axis whenever subjected to the x- or y- component of ground motion. The floor rotation, θ_j, as a result of force $V_{o,j}$ acting at the CM is:

$$\theta_j = \frac{\mathrm{M}_{v,j}}{K'_{z,j}} = \frac{-V_{o,j} \cdot \cos a \cdot e_y + V_{o,j} \cdot \sin a \cdot e_x}{K'_{z,j}} \tag{1a}$$

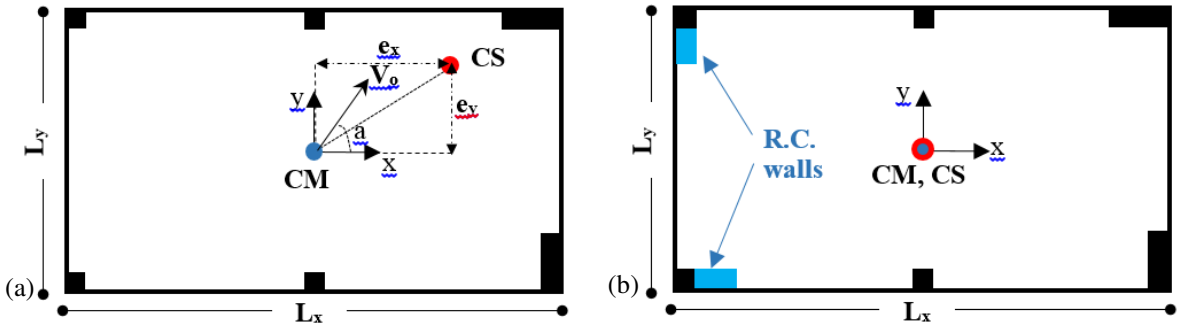

FIGURE 3 Plan layout (a) of the existing building; (b) of the retrofitted building (eccentricity elimination).

where $K_{z,j}^{/}$ is the rotational stiffness defined at the CS according to:

$$K_{z,j}^{/} = \sum_{i=1}^{n}\left[K_{y,i}\cdot(x_i - e_x)^2 + K_{x,i}\cdot(y_i - e_y)^2\right] \tag{1b}$$

and $K_{x,i}$, $K_{y,i}$ are the lateral stiffness of the individual floor elements and x_i, y_i is the distance of the geometrical center of each element from the origin xOy. The eigenvalue problem of the existing building whose solution provides the natural frequencies, ω_s, and modes, Φ_s, is described mathematically by:

$$\omega_s^2 \cdot \begin{bmatrix} \boldsymbol{m} & \boldsymbol{0} & \boldsymbol{0} \\ \boldsymbol{0} & \boldsymbol{m} & \boldsymbol{0} \\ \boldsymbol{0} & \boldsymbol{0} & \boldsymbol{J_m} \end{bmatrix} \cdot \begin{Bmatrix} \boldsymbol{\Phi_x} \\ \boldsymbol{\Phi_y} \\ \boldsymbol{\Phi_z} \end{Bmatrix} = \begin{bmatrix} \boldsymbol{K_x} & \boldsymbol{0} & -e_y \cdot \boldsymbol{K_x} \\ \boldsymbol{0} & \boldsymbol{K_y} & e_x \cdot \boldsymbol{K_y} \\ -e_y \cdot \boldsymbol{K_x} & e_x \cdot \boldsymbol{K_y} & \boldsymbol{K_z} \end{bmatrix} \cdot \begin{Bmatrix} \boldsymbol{\Phi_x} \\ \boldsymbol{\Phi_y} \\ \boldsymbol{\Phi_z} \end{Bmatrix} \tag{2}$$

where ω_s (s=x,y,z) is the natural frequency, $\mathbf{K_x}$, $\mathbf{K_y}$, $\mathbf{K_z}$ are the diagonal submatrices of the translational stiffness in x and y direction and of the rotational stiffness. $\mathbf{\Phi_s}^T=[\Phi_{s,1}, \Phi_{s,2},\ldots, \Phi_{s,N}]^T$ (s=x, y, z) are the mode shapes of the system. $\mathbf{m}$, $\mathbf{J_m}$ are the diagonal submatrices of the mass and moment of inertia.

The mode shapes are coupled through the stiffness matrix, K, because the stiffness properties are not symmetric about the x and y axes. The objective of retrofitting is to eliminate eccentricity so that $K_{x\theta}=K_{\theta x}=K_{y\theta}=K_{\theta y}=0$ (i.e., $e_x=e_y\approx 0$, i.e., move the CS to the CM, and thus $\theta\approx 0$ (Eq. (1a)), and to simultaneously increase the rotational stiffness, K_z, so that the torsional radius could receive higher values

than the radius of gyration, then the system would be uncoupled in x, y and z directions. This can be achieved by adding stiffness to the system in strategically selected positions at the periphery of the building as to minimize eccentricity and simultaneously increase torsional resistance (Fig. 3(b)). The translational and rotational stiffness of floor j of the strengthened system after the addition of m structural members (e.g., R.C. walls) are:

- Floor translational stiffness of the strengthened building:

$$K_{x,j}^{R} = \sum_{i=1}^{n} K_{x,i} + \sum_{p=1}^{m} K_{x,p} \;\; ; \;\; K_{y,j}^{R} = \sum_{i=1}^{n} K_{y,i} + \sum_{q=1}^{l} K_{y,q} \tag{3a}$$

- Floor rotational stiffness of the strengthened building:

$$K_{z,j}^{R} = \sum_{i=1}^{n} (K_{y,i} \cdot x_i^2 + K_{x,i} \cdot y_i^2) + 0.25 \cdot L_x^2 \cdot \sum_{q=1}^{l} K_{y,q}^{R} + 0.25 \cdot L_y^2 \cdot \sum_{p=1}^{m} K_{x,p}^{R} \tag{3b}$$

where $\sum_{p=1}^{m} K_{x,p}$ and $\sum_{q=1}^{l} K_{y,q}$ refer to the additional stiffness required as to remove any eccentricity of the floor plan.

Eq. (2) that describes the eigenvalue problem for the existing building is modified accordingly as to account for the effect of the additional stiffness that lead to elimination of eccentricity and enhancement of the torsional resistance:

$$\omega_s^2 \cdot \begin{bmatrix} \boldsymbol{m} & \boldsymbol{0} & \boldsymbol{0} \\ \boldsymbol{0} & \boldsymbol{m} & \boldsymbol{0} \\ \boldsymbol{0} & \boldsymbol{0} & \boldsymbol{J_m} \end{bmatrix} \cdot \begin{Bmatrix} \boldsymbol{\Phi_x^R} \\ \boldsymbol{\Phi_y^R} \\ \boldsymbol{\Phi_z^R} \end{Bmatrix} = \begin{bmatrix} \boldsymbol{K_x^R} & \boldsymbol{0} & \boldsymbol{0} \\ \boldsymbol{0} & \boldsymbol{K_y^R} & \boldsymbol{0} \\ \boldsymbol{0} & \boldsymbol{0} & \boldsymbol{K_z^R} \end{bmatrix} \cdot \begin{Bmatrix} \boldsymbol{\Phi_x^R} \\ \boldsymbol{\Phi_y^R} \\ \boldsymbol{\Phi_z^R} \end{Bmatrix} \tag{4}$$

where $\omega_s{}^R$ (s=x,y,z) is the natural frequency of the retrofitted system, $\mathbf{K_x^R}$, $\mathbf{K_y^R}$, $\mathbf{K_z^R}$ are the diagonal submatrices of the translational stiffness in x and y direction and of the rotational stiffness of the retrofitted system. $(\mathbf{\Phi_s^R})^T = [\Phi_{s,1}, \Phi_{s,2}, \ldots, \Phi_{s,N}]^T$ (s=x, y, z) are the mode shapes of the system. $\mathbf{m}$, $\mathbf{J_m}$ are the diagonal submatrices of the mass and moment of inertia. Thus, the three uncoupled equations that describe the eigenvalue problem are:

$$\omega_x^2 \cdot \boldsymbol{m} \cdot \boldsymbol{\Phi}_x^R = \boldsymbol{K}_x^R \cdot \boldsymbol{\Phi}_x^R ; \omega_y^2 \cdot \boldsymbol{m} \cdot \boldsymbol{\Phi}_y^R = \boldsymbol{K}_y^R \cdot \boldsymbol{\Phi}_y^R ; \ \omega_z^2 \cdot \boldsymbol{m} \cdot \boldsymbol{\Phi}_z^R = \boldsymbol{K}_z^R \cdot \boldsymbol{\Phi}_z^R \quad (5)$$

According to Eq. (5) the modified building (Fig. 3(b)) will response independently in the two lateral directions (torsional effects have been neglected) following the corresponding fundamental mode shapes.

In the proposed rehabilitation framework, deformation demand is quantified by interstorey drift throughout the building. The degree of stiffness irregularity along the height of the building, and the resulting local increase in the magnitude of demand (i.e., the magnitude of imposed interstorey drift (ID)), during an earthquake may be diagnosed by the morphology of the fundamental translational mode of vibration [Thermou et al., 2007]. The proposed methodology targets the systematic reduction of deformation demand, and in particular, the elimination of any tendency for localization of demand in parts of the structural system.

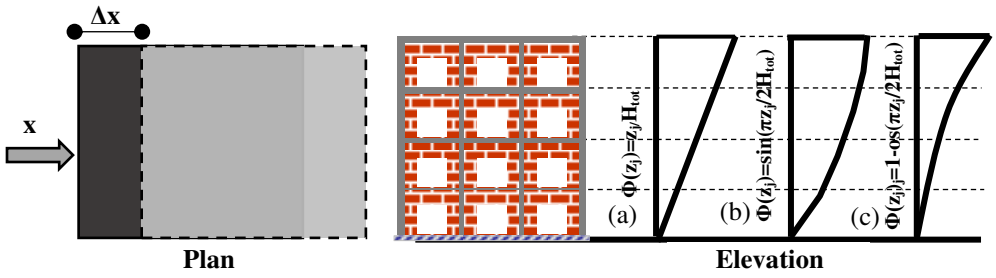

FIGURE 4 Lateral displacements profiles; (a) triangular; (b) shear; (c) flexural.

This objective is achieved by engineering the translational mode-shape of the structure, so as to optimize the distribution of interstorey drift (ID) according to the methodology developed by Thermou et al. [2007]. For example, a uniform distribution of ID would correspond to a linear first-mode shape (Fig. 4(a)) whereas a shear-type first mode is marked by higher increments in the lower floors, gradually decreasing toward the upper floors (Fig. 4(b)). The reverse pattern occurs in a flexural-type translational mode (Fig. 4(c)). In a reverse process of redesign, in which the desirable pattern of ID distribution prescribes the proper morphology of the fundamental mode shape, it is relatively straightforward to evaluate the pattern of stiffness distribution throughout the structure that is required to produce a desirable

translational mode. The necessary stiffness that is estimated from this process can be added to each floor through pertinent interventions, as required. Dimensioning and detailing of these interventions refer to the basic mechanics of reinforced concrete.

3.2 Stepwise presentation of the proposed methodology

The entire procedure is outlined by the following steps:

Step 1: Assessment of the existing building – The existing building is assessed at local (i.e., at member level) and global level (i.e., structural level). Flexural and shear resistance as well as chord rotation at yielding and at ultimate are calculated following the procedure described in EC8-Part III [2005] and the Greek Code for Interventions [GRECO, 2014]. The expressions utilized appear in Appendix A. The shear strength ratio, r_v ($=V_{R,j}/V_{y,j}\leq 1$), is defined which when is lower than unit premature failure due to shear is expected [Thermou and Pantazopoulou, 2011]. Moreover, the effective stiffness of the structural members is estimated. The structural regularity in plan is assessed by adopting the quantified criteria defined by EC8-Part I [2004]. The slenderness, λ ($=L_{max}/L_{min}$), of the building in plan should be less than 4.0 (L_{max} and L_{min} are the in plan dimensions of the building measured in orthogonal directions). The structural eccentricity in both directions x-x and y-y, $e_{o,x}$ and $e_{o,y}$, should be smaller than 30% of the torsional radius in both horizontal directions, r_x and r_y, respectively. The torsional radius for each direction of analysis x and y, r_x and r_y, should be larger than the radius of gyration, ℓ_s. The following conditions apply:

$$e_{oy} \leq 0.30 \cdot r_y \text{ and } r_y \geq \ell_s \text{ with } r_y = \sqrt{\frac{K_z^{R/}}{K_x}} \tag{6a}$$

$$e_{ox} \leq 0.30 \cdot r_x \text{ and } r_x \geq \ell_s \text{ with } r_x = \sqrt{\frac{K_z^{R/}}{K_y}} \tag{6b}$$

where $K_z^{R/}$ is the torsional stiffness of the retrofitted building (after the elimination of torsional effects) defined at the center of stiffness (CS). The center of stiffness is determined according to the procedure

provided by the Greek Annex of EC8-Part I [2004] with the determination of the fictitious elastic axis of multistorey buildings [Hellenic Seismic Code, 2000, Makarios and Anastasiadis, 1998a,b, Makarios, 2008]. For this purpose a spatial model of the building is required and elastic analysis with cracked cross sections is performed. Alternatively, eigenvalue analysis could also be performed for assessing the mode shapes and the influence of torsion.

Step 2: Elimination of the torsional sensitivity – The objective is to eliminate the effects of torsion in response. This could be easily accommodated with the addition of global intervention methods (e.g., infill R.C. walls, metallic cross braces) at the periphery of the building. The position of the added structural elements is selected as to minimize structural eccentricity (e_{ox}=e_{oy}≈0) and also to offer enough torsional stiffness, K_z^R (Eq. 4). The effect of the added structural members on the response of the building is assessed by eigenvalue analysis considering cracked cross sections. In case that the first two modes are translational with a mass participation factor close to 85% then the amount of added stiffness is considered sufficient.

Step 3: Controlling the distribution of interstorey drift

Target period: The target period of the retrofitted building, T_{target}, is defined. An acceptable range for selecting the target period value in retrofitting a flexible building may be defined by the code prescribed value [EC8, 2004] as the most stringent lower limit, and the period of the structure after solving the torsional behavior issues, as the upper, more lenient limit:

$$0.05 \cdot H_{tot}^{3/4} \le T_{target} < T_T \tag{7}$$

where H_{tot} is the total height of the building and T_T is the period of the building after the elimination of torsional response. Alternatively, T_{target} may be estimated as not to exceed a preset limit value described by the drift demand $\Theta_{u,target}$ of the structure according to the performance level selected [e.g. SEAOC, 1995; FEMA 356, 2000, Priestley and Kowalsky, 2000]. The drift demand at yielding is estimated $\Theta_{y,target}$(=

$\Theta_{u,target}/\mu$) after deciding on the ductility level, μ. The drift demand at yielding, $\Theta_{y,target}$, is related to the elastic spectral displacement demand by:

$$\Theta_{y,\text{target}} = S_d(T) \cdot \Gamma / H_{tot} \tag{8}$$

where $\Gamma=L^*/M^*$ is the participation factor with $L^*=\Sigma m_j \Phi_j$, $M^*=\Sigma m_i \Phi_j^2$, m_j is the mass at j^{th} floor and Φ_j is the shape value at floor j. If demand is defined according to Type I earthquake design spectra of the EN1998-1 (2004), then drift demand at yielding, $\Theta_{y,target}$, may be estimated from:

$$T_B \le T \le T_C: \ \Theta_{y,\text{target}} = 0.063 \cdot a_g \cdot S \cdot \eta \cdot T_{target}^2 \frac{\Gamma}{H_{tot}} \tag{9a}$$

$$T_C < T \le T_D: \Theta_{y,\text{target}} = 0.063 \cdot a_g \cdot S \cdot \eta \cdot T_C \cdot T_{target} \frac{\Gamma}{H_{tot}} \tag{9b}$$

where a_g is the design ground acceleration, T_B is the lower limit of the period of the constant spectral acceleration branch, T_C is the upper limit of the period of the constant spectral acceleration branch, T_D is the value defining the beginning of the constant displacement response range of the spectrum, S is the soil factor, η is the damping correction factor with a reference value of $\eta=1$ for 5% viscous damping, T_{target} is the target vibration period of the ESDOF system and H_{tot} is the total height of the building. The designer is free to select a target period which for a given ductility level will modify the target displacement. Moreover, attention should be paid to the cost of the intervention which increases as T_{target} is reduced getting closer to the stringent lower limit as suggested by [EC8-Part I, 2004].

Stiffness distribution along the height of the building: The Yield Point Spectra [Aschheim and Black, 2000] representation is utilized for definition of demand. The YPS are inelastic acceleration-yield displacement response spectra (ADRS) and can be generated from either a code-based format or a site-specific record. In current study, YPS are obtained from Type I elastic spectrum of EC8–Part I [2004]

after scaling down its x and y coordinates through pertinent q-μ-T relationships. The q-μ-T relationships used in current study are the one proposed by Vidic et al. [1994]:

$$q = (\mu - 1)\frac{T}{T_0} + 1; \quad \mathrm{T} \le \mathrm{T}_0 \tag{10a}$$

$$q = \mu; \quad \mathrm{T} > \mathrm{T}_0 \quad \text{where} \quad T_0 = 0.65 \cdot \mu^{0.3} \cdot T_c \le T_c \tag{10b}$$

where q is the behavior factor, μ is the ductility and T_C is the corner period at the plateau. The YPS for peak ground acceleration a_g= 0.36g, subsoil of class B with S = 1.20, spectral acceleration amplification factor for 5% viscous damping β_0= 2.50, with corner point periods defining the various spectrum regions equal to T_B=0.15s, T_C=0.50s and T_D=2.50s are presented in Fig. 5(a). For a target period and ductility level (e.g., T_{target}=0.5s and μ_{target}=2), the target displacement at yielding of the ESDOF, $\delta^*_{y,\ target}$, is estimated as shown in Fig. 5(b). A target ductility value, μ_{target}, between 2 and 3 may be considered achievable for retrofitted buildings.

Next, the target response shape, Φ_{target}, is selected. The driving consideration is the pursuit to obtain as nearly uniform as possible a distribution of drift demand. A more relaxed shape (leading to a more economical solution) may be used as well depending on the tolerance of damage localization in a single floor as well as the structural type of the building. Recent studies [e.g. Aslani and Miranda, 2005; Cardone, 2016, Cardone and Perrone, 2016], have revealed that damage associated to non-structural elements determines the larger part of the total repair cost (almost 80% of the expected annual loss) for substandard RC frame buildings. Hence, damage to non-structural members need also be considered by imposing limitations on the interstorey drift. For example, EC8-Part I [2004] refers to limits that are related to the seismic zone, the seismic hazard conditions, the protection of property objective, the type of the non-structural members (ductile or brittle) as well as to whether they interfere with the structural deformations.

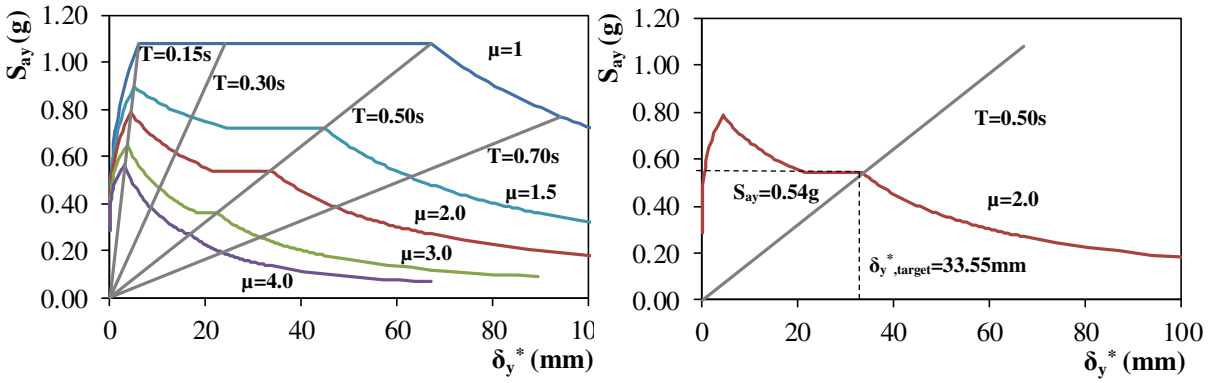

FIGURE 5 (a) Demand spectra for constant ductilities in ADRS format; (b) demand for T_{target}=0.5s and μ_{target}=2.

When considering structural vibration in the selected target response shape, the generalized (effective) SDOF properties of the structure are related to the target period and from there to the required secant-to-yield stiffness of the first floor, K_1, as follows [Thermou et al., 2007]:

$$K_1 = \frac{4\pi^2}{(T_{target})^2}\left(m \cdot w_1 \frac{\sum_{j=1}^{n} \Phi_j^2}{\sum_{j=1}^{n} w_i \cdot \Delta\Phi_j^2} \right) \tag{11}$$

where K_1 is the stiffness of the first storey, m is the typical storey mass, Φ_j is shape value at the j^{th} storey (N is the total number of storeys), $\Delta\Phi_j$ is the difference in shape between successive floors, T_{target} is the target period. Weighting factors, w_j, are utilized for the distribution of stiffness of the multi-degree-of-freedom (MDOF) along the height of the building [Thermou et al., 2007]. To derive the vector of weighting factors Rayleigh's method was used. The latter analysis converges to the fundamental mode shape that satisfies force equilibrium indirectly through energy conservation [Thermou et al., 2007]. The work-equivalent stiffness comprises contributions of the deformable elements in all floor levels; strain energy is associated with translational inter-storey drift for shear frame structures, and depends on tangential inter-storey drift in flexural wall-frame systems. The factor w_1 corresponds to the weighting

factor value at the first storey weighting factors. The values of the weighting factors for the triangular response in case of equal storey height for 2- to 8-storey buildings appear in Fig. 6(a). Eq. (11) may be further simplified in case of the triangular response shape and considering equal storey height to:

$$K_1 = \frac{4\pi^2}{(\mathrm{T}_{target})^2}\left(m \cdot w_1 \cdot \sum_{j=1}^{N} i\right) \tag{12}$$

The required stiffness in the j-th floor, K_j, associated with the selected target shape is obtained from:

$$\frac{K_j}{K_1} = \frac{w_j}{w_1} \tag{13}$$

Alternatively, the charts of Fig. 6(b) may be utilized directly. For example, for a four-storey building and a triangular target response shape $K_2/K_1=0.9$, $K_3/K_1=0.7$ and $K_4/K_1=0.4$. This procedure is repeated in both lateral directions. The additional stiffness required at each storey in both lateral directions, as for the lateral response shape to conform to the target shape, is equally distributed along the vertical members of the floor. In the selection of the vertical members to be strengthened attention should be paid as not to modify the center of stiffness.

Dimensioning and detailing: Each member of the j^{th} floor need be designed in order to satisfy the required stiffness, K_j, calculated using Eq. (13). Cross sectional dimensions of the retrofitted members (e.g., R.C. jackets) or the new added members (e.g., R.C. infill walls) is defined. The design of the retrofitted members should comply with the code provisions (e.g., minimum bar diameter, percentage of longitudinal reinforcement). Note that deviations from the required stiffness and thus from the target shape may be imperative due to construction limitations such as in cases that the stiffness of the existing floors already exceeds the required stiffness. The distribution of the added stiffness along the retrofitted members should not affect the center of stiffness as defined after the elimination of the torsional sensitivity at the first stage of the methodology. Deficiencies at local level leading to premature failure modes are addressed through local interventions at member level (e.g., FRP jacketing).

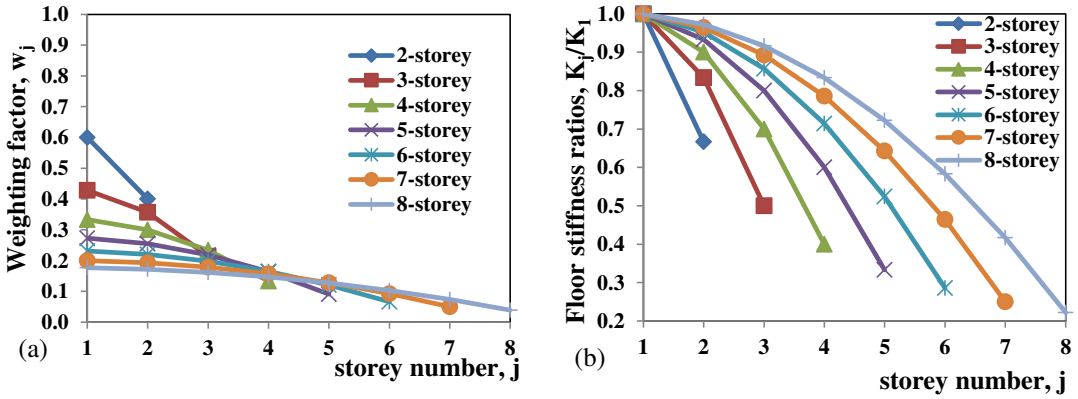

FIGURE 6 (a) Weighting factors and (b) floor stiffness ratio K_j/K_1 assuming equal storey height for the triangular response shape.

3.3 Limitations of the proposed retrofit design methodology

The optimum retrofit design scenario for substandard construction should provide a feasible solution from a structural point of view by considering the deficiencies at both local and global level and also estimate the impact of various performance indicators related to economic losses.

The proposed retrofit design methodology aims to eliminate the effects of torsion in response and limit the magnitude and distribution of interstorey drift demand in the building according to the selected target response shape. Within the conceptual framework of the proposed methodology, interstorey drift demand is used as an index of damage assessment which is directly related to the definition of the performance objectives of rehabilitation [Thermou et al., 2012b]. The retrofit solution provided by the proposed methodology corresponds to a specific scenario described by the target response shape, target ductility level and demand defined by the ADRS for a given hazard level. The proposed methodology does not provide any tools to evaluate economic losses related to the amount of damage the building may experience and the consequences of this damage including potential casualties, loss of use or occupancy, and repair and reconstruction costs. The provided retrofit solution could be assessed as a cost-effective one by using methodologies developed towards this direction. For example, the build loss estimation

methodology proposed by Aslani and Miranda [2005] and the FEMA P-58-1 [2012] methodology as applied to substandard RC building in the Mediterranean region by Cardone [2016], Cardone and Perrone [2016] could be used. The interstorey drift demand is the key element that can relate the proposed retrofit design methodology and methodologies referring to damage and loss assessment. The structure of the proposed methodology is such that could in a future version easily incorporate tools related to decision making. Thus, in step 3 of the proposed methodology various scenarios could be defined depending on the target periods, target response shapes, ductility levels and then assessed according to structural performance indices and performance indicators used on decision making.

4. Illustration of the proposed retrofit design methodology trough a real case study

The methodology described in section 3.2 is implemented in a three-storey residential R.C. building representative of the construction practice in Greece in the early 1970s. The building was designed for gravity loads [Royal Decree, 1954] and a low level of peak ground acceleration, pga =0.08g [Royal Decree, 1959]. Before the implementation of the proposed retrofit design methodology, a prerequisite step refers to the assessment of the existing building. The main objective is to check structural regularity in plan and elevation and identify any brittle failure that may jeopardize the structural stability in lateral deformation induced by future earthquake events. This step is crucial and the information collected will define the objectives of retrofitting.

4.1 Assessment of the existing building

A typical floor plan layout of the selected structure is shown in Fig. 7(a). The first storey (i.e., ground floor) has a commercial use (practically open ground floor due to shop windows) whereas the other two floors are used as residential apartments. The plan layout of the first storey is differentiated from that of the other two floors. The building featured various deficiencies such as low percentage of transverse reinforcement (stirrups with Ø6 mm nominal diameter at sparse arrangement s=250 mm with open legs),

insufficient anchorages, no stirrups in the beam-column joints, indirect supports (beam to beam connections) and structural irregularity in plan. The columns have a rectangular cross section with dimensions varying along the building's height, generally reducing by 5cm in each upper floor whereas the longitudinal reinforcement ranged between ρ_i=6.6‰ ÷ 10.3‰. Detailing regarding the column cross sections appears in Fig. 7(b). The geometry and the reinforcement detailing of R.C. walls followed the typical construction practice the provisions of the first Greek Seismic Code [Royal Decree, 1959]. The dimensions of the wall cross section were 1200 mm ÷ 2150 mm long by 150 mm ÷ 250 mm in width. The cross section geometry of the walls remained intact along the height of the building. The boundary elements were lightly reinforced by 4Ø12 mm longitudinal bars and the web reinforcement comprised of a dual mesh Ø8/250 mm. The total area ratio of the R.C. walls in each storey and in both directions of the existing R.C. building, ρ_w, was estimated equal to 0.53% ($=\Sigma A_w/A_{fi}$=1.68/317.85=0.53%). According to the relevant paragraph of the first Greek Seismic Code [Royal Decree, 1959] the R.C. walls will have to be arranged in such way as the total area of the R.C. walls in any storey in each direction of loading to be at least equal to 2‰ of the total floor plan area of the stories above. For the three storey building examined herein with a floor plan area of 317.85m^2, the minimum wall area required in the first floor would be 2×2‰×3×317.85=3.81 m^2. Hence, the required area ratio of walls according to the chart of Fig. 1(a) in the first storey is $\rho_{w,1}$=1.2% much higher than the provided one, indicating this building does not comply with the requirements of the code of that era. The longitudinal reinforcement area ratio ranged between 3.1‰ ÷ 14.7‰ approximately. Note that in a few beams three different bar diameters were placed (e.g., 10 mm, 12 mm and 16 mm). Transverse reinforcement followed the same pattern as in columns. The slab thickness was 0.10 m constant at all floors and was considered to offer diaphragmatic action. Concrete quality is B160 corresponding to a characteristic concrete compressive strength f_{ck} =10 MPa. Smooth bars with a mean stress at yield f_{ym}=250 MPa (StI according to DIN 1045 (1936)) were used for both longitudinal and transverse reinforcement.

The assessment at member level of the existing building followed the procedure described in EC8-Part III [2005] and the Greek Code for interventions [GRECO, 2014]. The chord rotation at yielding, $\theta_{y,j}$, and at ultimate, $\theta_{um,i}$, the flexural, $V_{y,i}$, and shear strength, $V_{R,i}$, of the existing columns, beams and walls were estimated according to the expressions that appear in Appendix A. In case of columns the shear strength ratio r_v ($=V_{R,i}/V_{y,i}\leq 1$) was lower than unit, indicating that premature failure is expected to occur in all the floors. The columns at the time of failure will have a chord rotation significantly reduced (almost half) of the chord rotation at yielding (Table 1). Referring to the walls no premature failure is anticipated since $r_v>1$ (Table1). Moreover, according to GRECO [2014] the effective stiffness at each end of a concrete member, EI_{eff}, may be computed from the yield moment, M_y, and the chord rotation at yielding at the end, θ_y, as:

$$EI_{eff,i} = M_{y,i} L_s / 3\theta_{y,i} \tag{14}$$

In this study, it is assumed that the columns of each storey are fixed in both ends whereas walls are fixed only at the base behaving thus as cantilevers. Thus, the shear span for the columns is equal to half the clear storey height ($L_s=h_{cl}/2$) whereas for the walls it was taken equal to 2/3 of the total height of the building ($L_s=2H_{tot}/3$). Eqs. 15 are used for estimating the stiffness, K_j, at member level. The total stiffness of each floor, K_j ($=\Sigma K_i$), is obtained by direct summation of the stiffness of the individual vertical members of each floor (since they are considered to function as a sequence of springs in parallel) and presented in Table 2:

For columns: $$K_i = M_{y,i} / (2 \cdot \theta_{y,i} \cdot L_s^2) \tag{15a}$$

For walls: $$K_i = M_{y,i} / \left(\theta_{y,i} \cdot L_s^2\right) \tag{15b}$$

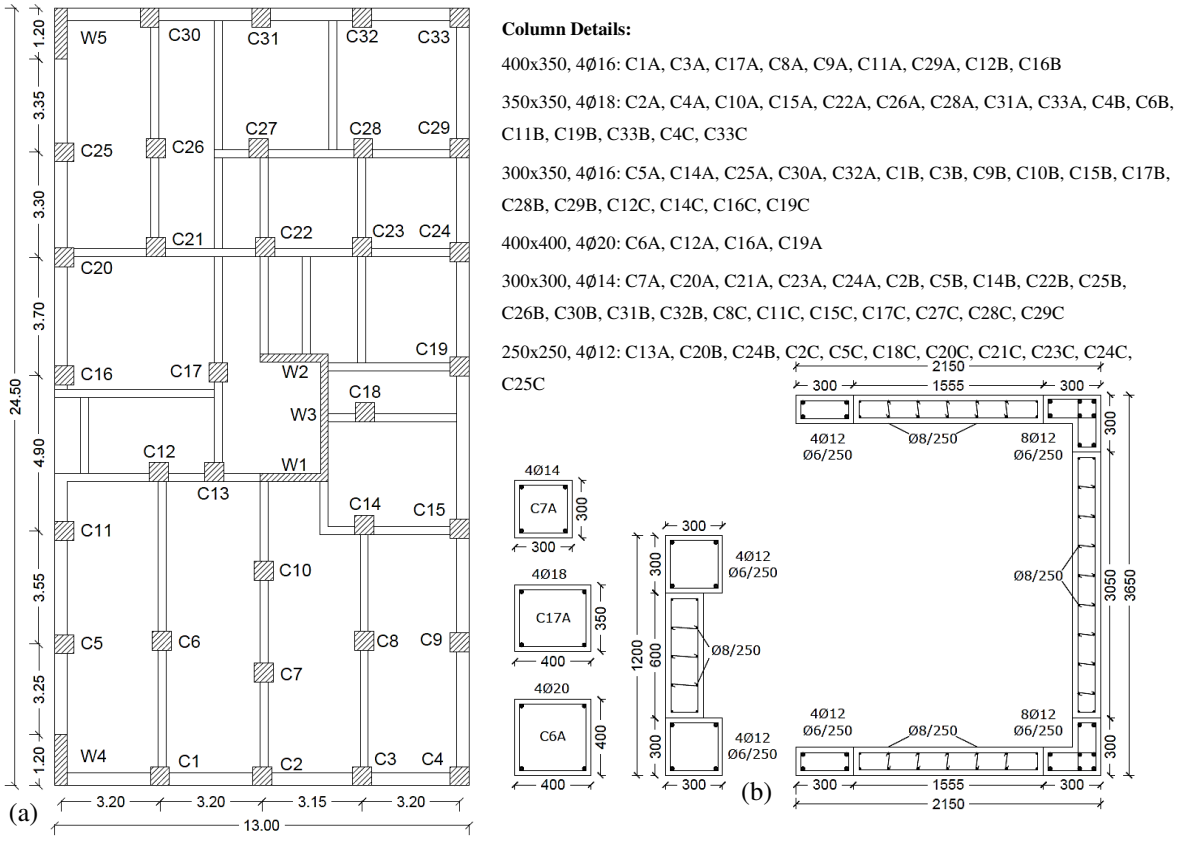

FIGURE 7 (a) Plan configuration of 1st storey of the existing building; (b) Cross-sectional detailing of columns and walls**.**

For the needs of performing the structural regularity check in plan as well as the eigenvalue analysis, a finite element model was developed using the SAP2000, version 15 [Computers and Structures Inc. (CSI), 2012]. Columns, walls and beams were modeled as elastic elements with an effective stiffness calculated according to Eq. (14). More details regarding the modeling process are presented in detail in section 4.4.1. The structural regularity in plan and elevation is checked according to the quantified criteria of Chapter 4 of EC8-Part I [2004]. The slenderness λ ($=L_{max}/L_{min}$) is 1.9, thus less than 4 ($\lambda=1.9<4$). The structural eccentricity in both directions, e_{ox} and e_{oy}, is smaller than 30% of the torsional radius (Table 3), whereas in both directions the torsional radius, r_x and r_y, is smaller than the radius of gyration (Table 3). Thus, the criteria described by Eqs. 6 are not satisfied and the building is characterized as irregular in plan in both

directions. Contrariwise, all lateral load resisting system run without interruption from the foundation to the top of the building. The modal response parameters of the existing building are presented in Table 4.

TABLE 1 Average values of the chord rotation at yielding, at ultimate and shear resistance of the vertical members.

Floor		$\theta_{y,col}^{flex*}$ (%)	$\theta_{u,col}^{flex*}$ (%)	$V_{shear,c}$ (kN)	V_y (kN)	$r_v=V_{shear,c}/V_y\leq1$	Failure	$\theta_{fail}^{*}=v\cdot\theta_{y,col}^{flex}$ (%)
1	Columns (C1-C33)	0.75	3.70	15.97	19.12	0.83	Shear	0.63
2		0.65	3.42	15.93	20.69	0.77	Shear	0.50
3		0.67	3.63	10.28	14.88	0.69	Shear	0.46
		$\theta_{y,wall}$ (%)	$\theta_{u,wall}$ (%)	$V_{shear,w}$ (kN)	V_y (kN)	$r_v=V_{shear,w}/V_y\leq1$	Failure	$\theta_{fail}=v\cdot\theta_{y,wall}^{flex}$ (%)
Walls	direction x-x (W1-W2)	0.32	3.26	652.87	50.68	1	Flexure	-
	direction y-y (W3-W5)	0.40	3.54	658.69	52.49	1	Flexure	-

* The values are calculated in both directions x-x, y-y due to the rectangle cross section

TABLE 2 Stiffness of each i storey at each direction.

Storey	Stiffness, K_j (kN/m)	
	direction x	direction y
1	27539.9	30463.3
2	51175.0	55541.0
3	41193.8	42351.0

TABLE 3 Check of structural regularity in plan.

Direction x					
$e_{ox}<$	0.30 r_x	check	$r_x>$	l_s	check
1.45	1.54	ok	5.14	7.99	not ok
Conclusion: irregular in plan					
Direction y					
$e_{oy}<$	0.30 r_y	check	$r_y>$	l_s	check
0.09	2.17	ok	7.24	7.99	not ok
Conclusion: irregular in plan					

TABLE 4 Elastic periods and modal participation mass ratios of the existing building.

No.	Period (sec)	Modal Participation Mass Ratio (%)		
		Ux	Uy	Rz
1	0.95	0.00	4.10	90.55
2	0.72	88.94	0.00	0.00
3	0.48	0.00	89.18	5.19

4.2 Elimination of torsional sensitivity

The main objective is to increase torsional resistance and minimize structural eccentricities in both directions in order for the building to respond in an uncoupled mode when subjected to lateral loading. For this purpose, stiffness is added at the periphery of the building in strategically selected locations as to minimize structural eccentricities. From among the various global interventions methods, the addition of R.C. infill walls was considered as being the most effective one in increasing significantly the lateral stiffness. The bays selected for the construction of the R.C. infill wall are depicted in Fig. 8(a) (R.C. infill walls: W6 - W9). The existing R.C. columns were incorporated in the infill walls as boundary elements after being jacketed (Fig. 8(b)). The width of the shear walls was such as to allow the vertical reinforcement of the web of the wall to pass by the beams of the infilled frames. The monolithicity of the infilled R.C. wall with the surrounding frame was secured by connecting dowels placed between the old and the new components (columns and beams) [GRECO, 2014]. The effective stiffness of the added shear walls was such as to minimize structural eccentricities in each direction. The addition of W6-W9 walls (Fig. 8(a)) increased significantly the area ratio of the R.C. walls in all the storeys and in both directions to 1.09%. The stiffness contribution of all the vertical elements were estimated according to Eqs.15. The dimensions of the infill walls along with their reinforcing detailing and their stiffness contribution are shown in Table 5. The materials selected for the new R.C. elements were a concrete with a characteristic strength of f_{ck}=30 MPa and steel with a characteristic yield strength f_{yk}=500 MPa. Dimensioning and detailing of the infill walls followed Chapter 5 of EC8-Part I [2004]. The code minima imposed

limitations in the design of the new members and those limitations guided the retrofit solution. Eigenvalue analysis was performed with the modeling assumptions presented in section 4.4. The participation mass ratios of the building after the addition of W6-W9 walls verify that torsional sensitivity was eliminated (Table 6).

TABLE 5 Dimensions and reinforcing details of the R.C. infill walls.

R.C. Walls								
R.C. Walls	b_x (mm)	b_y (mm)	Web Reinforcement (mm)	Stirrups (mm)	$\rho_{f,j}^{*}$ (%)	$\rho_{w,j}^{*}$ (%)	K_x (kN/m)	K_y (kN/m)
W6	200	2450	#Ø10/200	Ø10/80	1.07 (4Ø24&4Ø16)	0.25	0	14340.4
W7	200	2450	#Ø10/200	Ø10/80	0.60 (4Ø12&4Ø18)	0.25	0	8927.2
W8	2050	200	#Ø10/200	Ø10/80	0.69 (4Ø14&4Ø16)	0.22	6127.4	0
W9	2050	200	#Ø10/200	Ø10/80	0.69 (4Ø14&4Ø16)	0.22	6113.8	0

*ρ_{fj}: reinforcement ratio of boundary elements; $\rho_{w,j}$: vertical web reinforcement ratio

TABLE 6 Elastic periods and modal participation mass ratios of the building after the addition of the R.C. infill walls

No.	Periods (sec)	Modal Participation Mass Ratio (%)		
		Ux	Uy	Rz
1	0.52	88.03	0.00	0.11
2	0.39	0.03	83.49	0.99
3	0.36	0.12	0.75	81.28

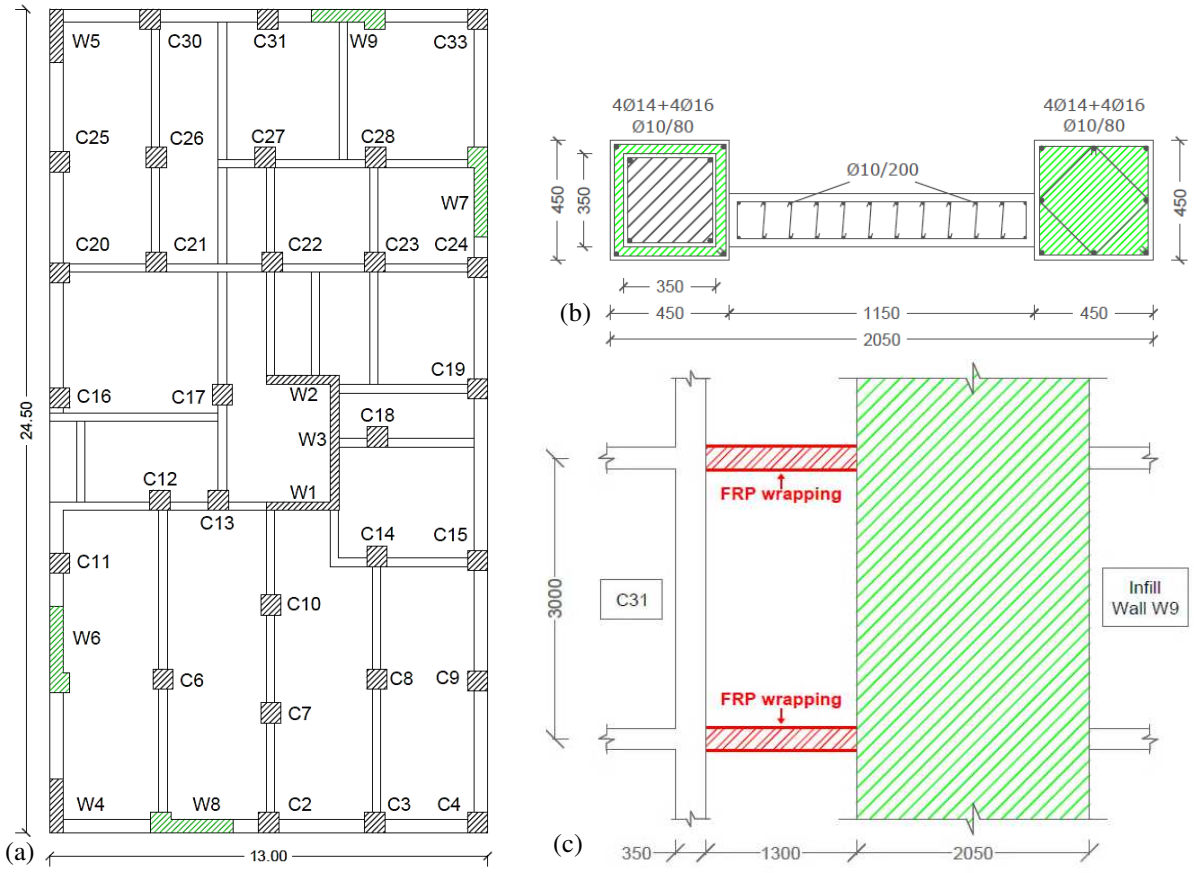

FIGURE 8 Elimination of the torsional sensitivity through the addition of the W6-W9 infill walls at the perimeter of the building; (a) plan layout of the retrofitted building in design phase I (elimination of torsional sensitivity); (b) cross-sectional detailing of the infill wall W9; (c) elevation view of the infilled wall bay.

4.3 Strengthening for a target interstorey drift

Once the torsional effects have been eliminated, the target value for the fundamental period of the buidling, T_{target}, and the target shape, Φ_{target}, are selected. The target period, T_{target}, will recceive a value between the following upper and lower limits:

$$0.05 \cdot H_{tot}^{3/4} = 0.05 \cdot 10.5^{3/4} = 0.29\text{s} \le T_{target} < T_{\inf,w} = \begin{Bmatrix} 0.52\text{s for x-x} \\ 0.39\text{s for y-y} \end{Bmatrix}$$

The lower limit of the period represents the code prescribed value, H_{tot} (=10.5m) is the total height of the building and $T_{inf,w}$ refers to the period of the translational mode after the addition of wall W6-W9 for the elimination of the torsional effects. Any target period between the lower and upper limit may be selected and from there the target stiffness distribution heightwise could be estimated. Its obvious that the the influence of stiffnes distribution of the existing building on the resulting lateral response shape after retrofitting will be high as long as the required addition of stiffness along the height of the building is low or in some cases when the stiffness of the existing building in one specific storey is higher than the target one. Thus, it is required to select such a value of target period that will allow for addition of a certain amount of stiffness along the height of the building as to respond according to the target shape. Based on the above, the target periods selected were 0.41s and 0.37s in x-x and y-y direction, respectively. The target ductility level was assumed equal to 2 which is considered a realistic scenario for substandard buildings. The target stiffness of each floor is determined through the use of the weighting factors [Thermou et al., 2007]. The three-storey building (MDOF system) with storey mass m=138.24t and triangular response shape is transformed to the corresponding ESDOF system with the following characteristics: $M^*=\Sigma m_j\Phi_j^2=230.79$t; $L^*=\Sigma m_j\Phi_j=$ 291.96t; $\Gamma=L^*/M^*=$ 1.27. The demand in all cases is defined by the Yield Point Spectra [Aschheim and Black, 2000] representation derived from Type I elastic spectrum of EC8-Part I [2004] and the q-μ-T relationships of Vidic et al. [1994].

The YPS depicted in Fig. 9 were defined for peak ground acceleration a_g= 0.36g, subsoil of class B with S = 1.20, β_0 = 2.50, with corner point periods defining the various spectrum regions equal to T_B=0.15s, T_C=0.50s and T_D=2.50s. Thus, given the target period in x and y direction, $T_{x,target}$=0.41s and $T_{x,target}$=0.37s, the target displacement at yield of the ESDOF system is estimated through the YPS equal to $\delta^*_{y,\ target,x}$= 22.56 mm and $\delta^*_{y,\ target,y}$=19.09mm, respectively (Fig. 9(a)). The target drift at yielding of the MDOF system in the x and y direction is $\Theta_{y,target,x}=\delta^*_{y,\ target,x}\cdot\Gamma/H_{tot}=0.27\%$ and $\Theta_{y,target,y}=\delta^*_{y,\ target,y}\cdot\Gamma/H_{tot}=0.23\%$, respectively. The target drift values estimated are in the range of 0.25% which is the drift at yielding expected to occur in case of RC wall-type structures [Thermou et al. 2007]. The weighting

factors for the three-storey building receive the values w_1=0.345, w_2=0.414, w_3=0.241. Then, the stiffness at the first storey in x-direction is calculated according to Eq.12, K_1=67211.37 kN/m. The stiffness of the second and third storey in x-direction are calculated based on Eq. (13), K_2=80653.64 kN/m; K_3=46950.55 kN/m. The same procedure for determining the stiffness demand in the floors is followed in the y direction (Table 7).

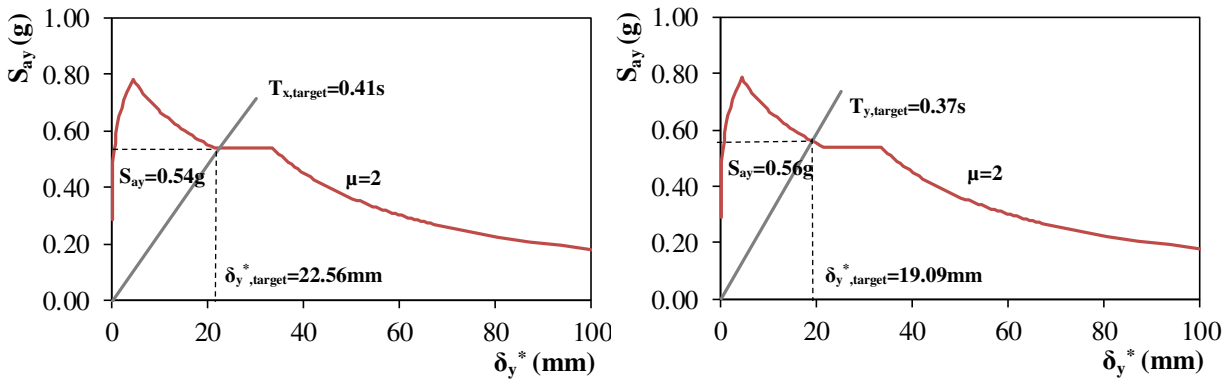

FIGURE 9 Demand for the adopted retrofit scenario in (a) direction x and (b) direction y.

Table 7 presents information related to the stiffness of the building at each design phase. The required stiffness distribution along the height of the building for the target response shape is also presented. It is observed that only in the first and second floor stiffness addition is required, whereas in the third floor the stiffness of the existing building after the elimination of torsion is already higher than the required stiffness for the target response shape. The latter implies that even in the case that the stiffness in the first and second storey are increased as to comply with the stiffness corresponding to the target response, the resulting lateral response shape would slightly deviate from the target one. It was decided to modify the stiffness of the first and second storey by the addition of R.C. jackets (i.e., longitudinal bars pass through holes drilled in the slab and anchored in the third storey). The columns to be jacketed are depicted by red color in Fig. 10(a). The selection of this specific group of columns and the distribution of the target added stiffness along them did not affect the center of stiffness as defined after the addition of W6-W9 walls. The same materials utilized for the walls were used for the columns' jackets. Details regarding

dimensioning of the R.C. jacketed members appears in Table B1 (Appendix B). The proposed retrofit solution leads to a lateral response shape very close to the target one as seen in Fig. 10(b)–(c) after applying the Rayleigh iterative method. The addition of the R.C. jackets in the first two floors managed to decrease the interstorey drift demand and lead to equal distribution of drift along the height of the building. Deficiencies at local level leading to premature failure modes will be addressed by FRP jacketing.

TABLE 7 Required stiffness for the correction of the response shape in x and y direction.

Stiffness in x direction, K_x (kN)				
Storey	Torsionally balanced building	Required Stiffness for target shape	Added stiffness (Design of R.C. jackets)	Stiffness at the end of the retrofit design
1	37391.42	67211.37	29710.25	67101.66
2	58234.98	80653.64	23343.24	81578.22
3	49735.74	46950.55	0.00	49735.74
Stiffness in y direction, K_y (kN)				
Storey	Torsionally balanced building	Required Stiffness for target shape	Added stiffness (Design of R.C. jackets)	Stiffness at the end of the retrofit design
1	51085.18	82529.08	31231.80	82316.98
2	73524.81	99034.89	25572.61	99097.43
3	62277.42	57650.75	0.00	62277.42

4.4 Assessment of the retrofit option

4.4.1 Modelling assumptions

The retrofitted building of Fig. 10(a) is assessed with the help of SAP2000 version 15 [Computers and Structures Inc. (CSI), 2012] finite element program. In case of eigenvalue analysis, which is considered in steps 1 and 2 of the proposed methodology, columns, walls and beams are modeled as elastic frame elements with an effective stiffness calculated according to Eq. (14). It is assumed that the contribution of the slabs to beam stiffness and strength is reflected by the effective width of the T-section. Mass was distributed to the beam-column joints whereas diaphragm action was taken into account using default diaphragm constraints.

For the needs of inelastic static analyses (pushover analyses) Mander's stress -strain model was used for confined and unconfined concrete [Mander et al., 1998] whereas a bilinear elasto-plastic model was used for steel. Columns and beams are modelled as frame elements with plastic hinges assigned at their ends. R.C. walls are modeled as frames elements connected at the floor level with beams by rigid end offsets, whereas plastic hinges were assigned at the base of the wall. Rigid elements are placed at beam-column joints thus preventing plastic hinge formation in the joints. Fully-fixed boundary conditions are adopted at the base of the building. Each plastic hinge is modeled as a discrete point hinge. In the present work user-defined moment hinges (M2 hinges in x and M3 hinges in y direction) are assigned at beams ends the behavior of which are described by moment – rotation (M-θ) diagrams. The moment and chord rotation at yielding and at ultimate were calculated based on the EC8-Part III [2005] and GRECO [2014] and verified by the cross section analysis section program Response 2000 [Bentz, 2000]. In case of columns and walls the automatic Caltrans hinges (P-M2-M3 hinges) are assigned which are based on the 3D interaction (yield) surface which defines coupling between axial and biaxial-bending behaviors.

4.4.2 Eigenvalue and pushover analyses

Eigenvalue analysis of the retrofit is performed and the modal response parameters are presented in Table 8. The intervention methods selected to be applied (R.C. infill walls at the perimeter of the building and the addition of R.C. jackets to existing columns (Fig. 10(a)) modified substantially the response. The first two modes are considered purely translational (the participation mass ratio is above 85%, Table 8). The periods of the first two modes are very close to the target ones. The lateral response shapes of the retrofitted building based on the results of modal analysis using SAP2000 version 15 [Computers and Structures Inc. (CSI), 2012] and the Rayleigh method are compared to the ones corresponding to the triangular response shape in Fig. 11(a)–(b). It is observed that the retrofit design methodology succeeded in providing a uniform distribution of damage between the floors of the retrofitted building.

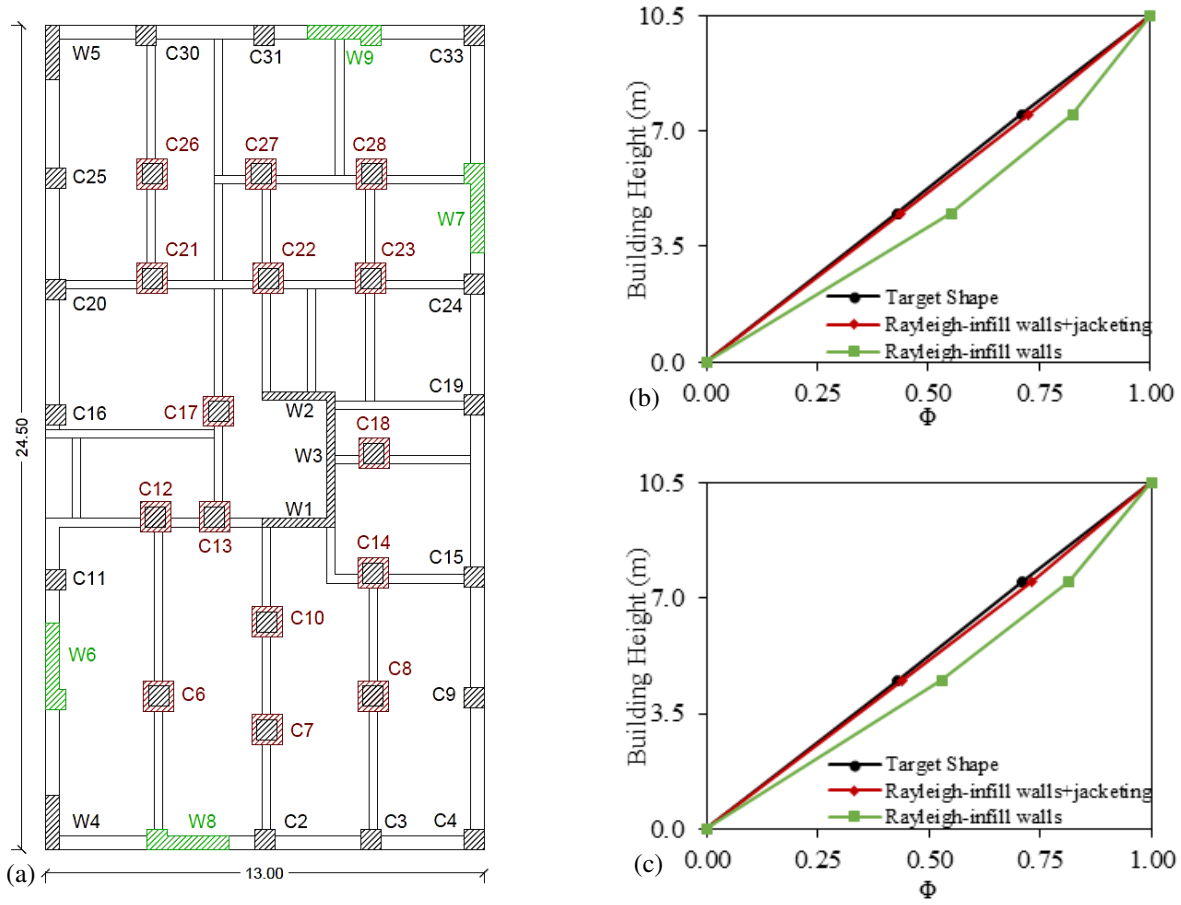

FIGURE 10 (a) Retrofit solution according to the proposed methodology; (i) addition of walls W6-W9 for elimination of torsional effects and (ii) strengthening for a target response shape through R.C. jacketing. Check of the vibration shape of the retrofitted building according to the Rayleigh Method (b) along the x-x axis (c) y-y axis.

TABLE 8 Elastic periods and modal participation mass ratios of the retrofitted building.

No.	Periods (sec)	Modal Participation Mass Ratio (%)		
		Ux	Uy	Rz
1	0.49	88.10	0.00	0.16
2	0.37	0.01	87.58	0.41
3	0.35	0.19	0.77	85.52

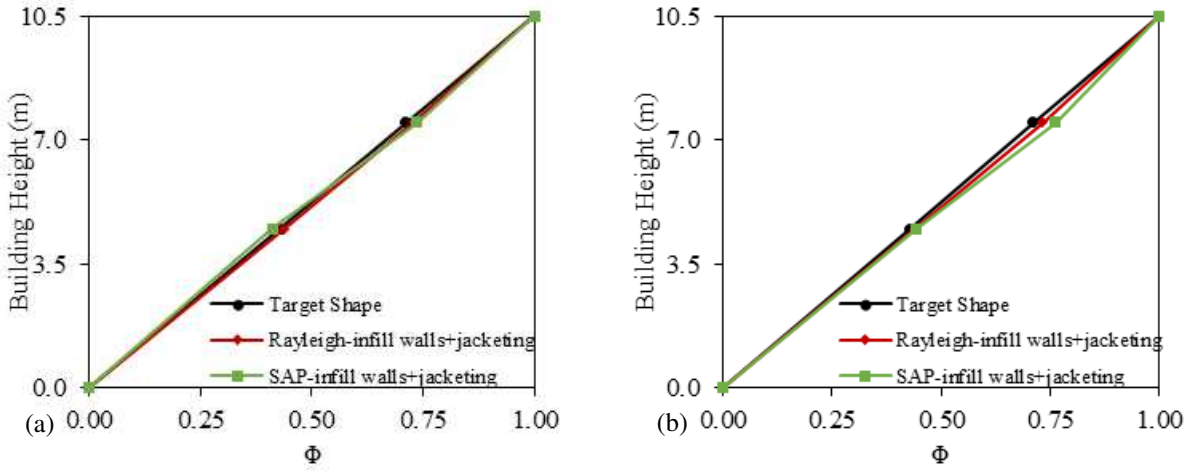

FIGURE 11 Vibration shape of the retrofitted building after the completion of the retrofit design according to Rayleigh method and SAP2000 results; (a) direction x; (b) direction y.

The dimensionless capacity curves $V/W_{G+0.3Q}$ versus Θ (i.e., base shear, V, normalized with respect to the weight of the building, $W_{(G+0.3Q)}$, versus roof displacement, Δ, normalized with respect to the total height of the building H_{tot}) are depicted in Fig. 12 for the uniform distribution of lateral load (i.e., for the most unfavorable load pattern). The black colored curves correspond to the capacity curve of the building after the addition of the R.C. walls, whereas the red colored curves correspond to the capacity curves after the addition of both R.C. walls and R.C. jackets (Fig. 12). The sequence of plastic hinge development revealed that plastic hinges formed first at the base of the R.C. walls in both directions of loading. The drift at which R.C. walls reached first yielding is defined by the blue square dots in Fig. 13 indicating the state of global yielding. The red circular dots that appear in Fig. 13 correspond to the ultimate state of the structure. The interstorey drift profiles at the global yielding (blue square dot in Fig. 13) and at ultimate (red circular dot in Fig. 13) in both x-x directions and y-y directions are shown in Fig. 14.

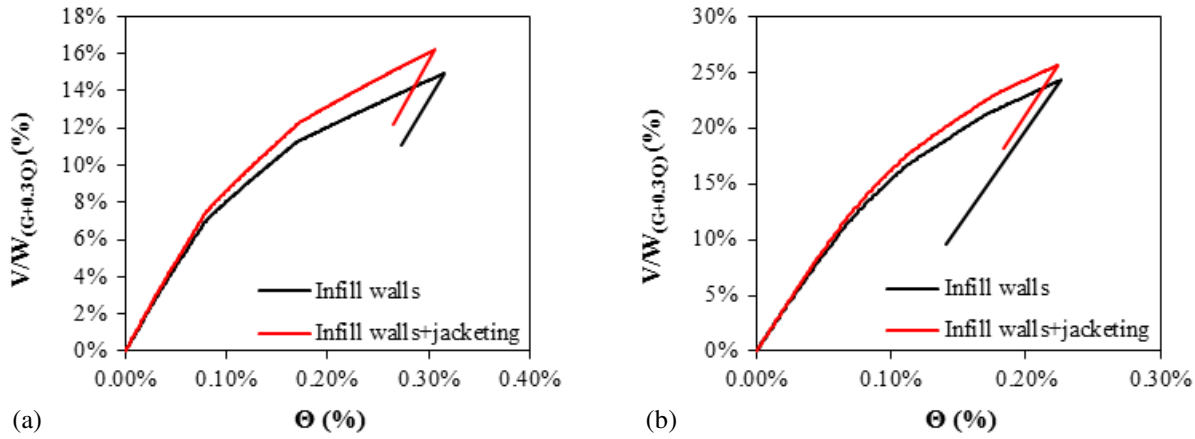

FIGURE 12 Comparison of the capacity curves before and after the addition of the R.C. jackets to selected existing columns in the first and second story: (a) direction x and (b) direction y.

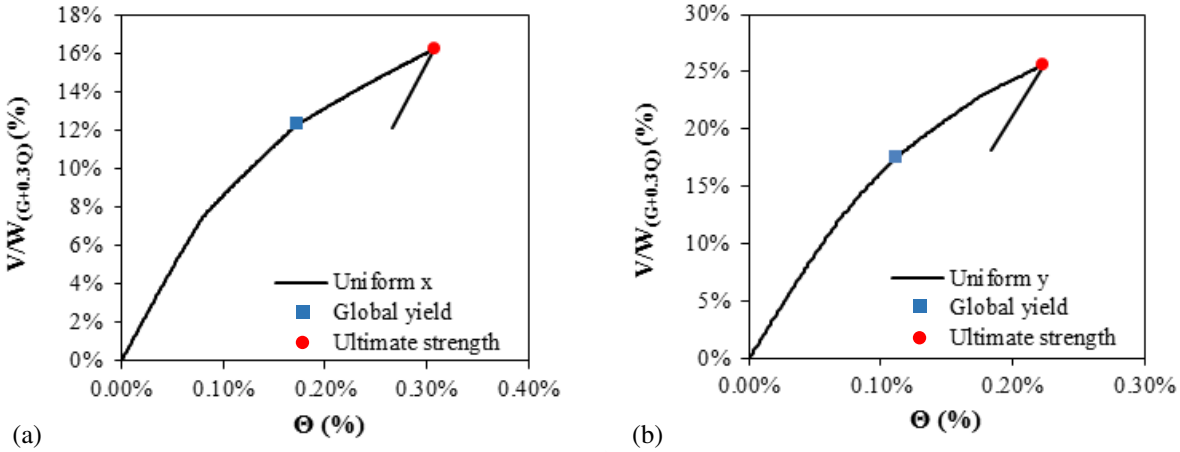

FIGURE 13 Calculated base shear vs top displacement for the retrofit solution; (a) direction x; (b) direction y.

The proposed retrofit design methodology managed to provide an almost uniform distribution of interstorey drift along the height of the building both in the yielding (Fig. 14(a)) and in the post yielding region (Fig. 14(b)). Minor deviations from the target response shape are justified and considered acceptable since in case of existing buildings a predefined distribution of stiffness along their heights exists and imposes limitations to future stiffness modifications heightwise as dictated by the target response shape. The drift at global yielding in x-x, $\Theta_{y,x}$, and y-y direction, $\Theta_{y,y}$, receives values equal to

0.17% and 0.11% (Fig. 13), respectively, which if compared to the target drift values at yielding ($\Theta_{y,target,x}$=0.27% and $\Theta_{y,target,y}$=0.25%) lead to the conclusion that the adopted retrofit solution is assessed as stiffer with the help of more detailed analysis where inelasticity of the system is considered. The outcome is on the safe side since lateral drift is further controlled and thus damage is limited. The estimated displacement ductility in both directions (x-x direction: $\mu_{\Delta,x}$=1.8, y-y direction: $\mu_{\Delta,y}$=2) satisfies the target one, $\mu_{\Delta,target}$=2.

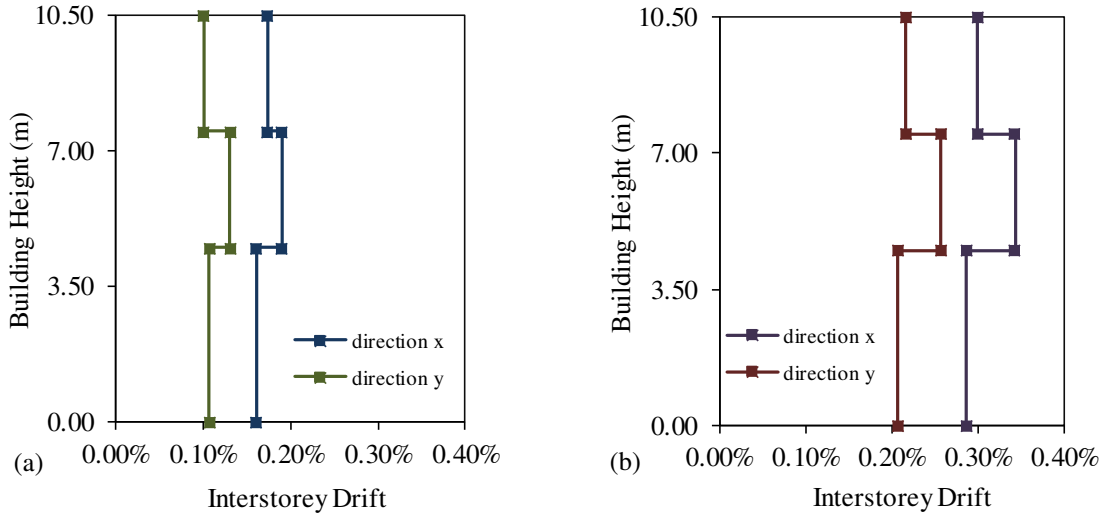

FIGURE 14 Interstorey drift ratio of the retrofitted building in the direction x and y; (a) global yield point; (b) ultimate strength.

5. Conclusions

This paper presented a retrofit design methodology for the seismic upgrading of rotationally sensitive existing R.C. buildings. The proposed methodology aims to modify substantially the response by minimizing structural eccentricities and simultaneously increasing torsional resistance and stiffness. For this purpose, stiffness is added through the adoption of global intervention methods at the periphery of the building so as to provide a building symmetric in plan and torsionally balanced. The lateral response shape in the two orthogonal axes (x-x and y-y) is further modified as to comply with the target response shape.

This is achieved by a weighted distribution of additional stiffness along the height of the building. The proposed methodology was implemented to a three-storey building constructed in the early 1970s in North Greece. The validity of the proposed methodology was assessed by carrying out inelastic analyses with the use of a three-dimensional finite element model of the retrofitted structure. The results indicate the efficiency of the proposed design methodology for the seismic upgrading of existing torsionally unbalanced R.C. buildings.

References

Applied Technology Council (ATC), FEMA P-58. [2012] Next-generation seismic performance assessment for buildings, Volume 1 and Volume, Federal Emergency Management Agency, Washington, D.C.

ASCE, 2000, Prestandard and Commentary for the Seismic Rehabilitation of Buildings, FEMA 356 Report, prepared by the American Society of Civil Engineers for the Federal Emergency Management Agency, Washington, D.C.

Aschheim, M.A. and Black, E.F. [2000] "Yield point spectra for seismic design and rehabilitation", Earthquake Spectra, 16(2), 317-336.

Aslani, H. and Miranda, E. [2005] "Probabilistic earthquake loss estimation and loss disaggregation in buildings", Report No. 157, John A. Blume Earthquake Engineering Center, Stanford University.

Bentz, E. C. [2000] "Sectional analysis of reinforced concrete members." PhD thesis, Department of Civil Engineering, University of Toronto, 187.

Calvi, G.M. [2013] "Choices and criteria for seismic strengthening", Journal of Earthquake Engineering, 17(6), 769-802.

Cardone, D. [2016] "Fragility curves and loss functions for RC structural components with smooth rebars", Earthquake and Structures, 10(5), 1181-1212.

Cardone, D., Perrone, G. [2016] "Damage and Loss Assessment of Pre-70 RC Frame Buildings with FEMA P-58", Journal of Earthquake Engineering, DOI: 10.1080/ 13632469.2016.1149893.

Computers and Structures Inc. (CSI) [2012] SAP 2000 – Nonlinear version 15, user's reference manual. Berkeley, California, USA.

Deutsches Institut für Normung [German Standards Institute] (DIN). Beton und Stahlbetonbau: Bemessung und Ausführung. DIN 1045, Berlin, 1936.

EAK 2000, Hellenic Seismic Code, Ministry of Environment, Planning and Public Works 2000, Athens, Greece (in Greek), 2000.

Eurocode 8 [2004] Design of structures for earthquake resistance - Part I: General Rules, seismic actions and rules for buildings, EN1998-1-2004: E, European Committee for Standardization (CEN). Brussels.

Eurocode 8 [2005] Design of structures for earthquake resistance. Part III: Assessment and retrofitting of buildings, EN 1998-3:2005(E), European Committee for Standardization (CEN). Brussels.

Fajfar, P. [1999] "Capacity spectrum method based on inelastic demand spectra", Earthquake Engineering and Structural Dynamics, 28, 979-993.

Greek Code for Interventions (GRECO) [2014] Earthquake Planning and Protection Organization, Athens.

Makarios T. [2008] "Practical calculation of the torsional stiffness radius of multistorey tall buildings", The Structural Design of Tall and Special Buildings, 17, 39-65.

Makarios T. and Anastassiadis K. [1998] "Real and fictitious elastic axes of multi-storey buildings: Theory", The Structural Design of Tall Buildings, 7, 33-55.

Makarios T. and Anastassiadis K. [1998] "Real and fictitious elastic axes of multi-storey buildings: Theory", The Structural Design of Tall Buildings, 7, 57-71.

Mander J.B., Priestley M.J.N. and Park R. [1988] "Theoretical stress-strain model for confined concrete", Journal of Structural Engineering, 114(8), 1804-1826.

Mazza, F. [2015] "Comparative study of the seismic response of RC framed buildings retrofitted using modern techniques", Earthquakes and Structures, 9(1), 29-48.

Pardalopoulos, S. and Pantazopoulou, S.J. [2011] "Spatial displacement patterns of R.C. buildings under seismic loads", in Computational Methods in Earthquake Engineering, Computational Methods in Applied Sciences 21, ed. M. Papadrakakis et al., Springer, pp. 123-145.

Priestley, M. J. N. and Kowalsky, M. J. [2000] "Direct displacement-based seismic design of concrete buildings", Bulletin, New Zealand National Society for Earthquake Engineering 33(4), 421-444.

Royal Decree [1954] Design regulation of reinforced concrete buildings works, Royal Decree (18.2/26.07.1954), Ministry of Public Works, Greece.

Royal Decree [1959] Earthquake design regulation of buildings works, Royal Decree (26.2.1959), Ministry of Public Works, Greece.

SEAOC [1995] Performance Based Seismic Engineering of Buildings, Vision 2000 Committee, Structural Engineers Association of California, Sacramento, California.

Thermou, G.E. and Elnashai, A.S. [2006] "Seismic retrofit schemes for R.C. structures and local-global consequences", Progress in Structural Engineering and Materials, 8(1), 1-15.

Thermou, G.E., and Pantazopoulou, S.J. [2011] "Assessment indices for the seismic vulnerability of existing RC buildings", Journal of Earthquake Engineering and Structural Dynamics, 40 (3), 293-313.

Thermou, G.E., Elnashai, A.S. and Pantazopoulou, S.J. [2012a] "Retrofit yield spectra spectra-a practical device in seismic rehabilitation", Earthquake and Structures, 3(2), 141-168.

Thermou, G.E., Pantazopoulou, S.J. and Elnashai, A.S. [2007] "Design methodology for seismic upgrading of substandard R.C. structures", Journal of Earthquake Engineering, 4(11), 582-606.

Thermou, G.E., Pantazopoulou, S.J. and Elnashai, A.S. [2012b] "Global interventions for seismic upgrading of substandard R.C. buildings", Journal of Structural Engineering, 138(3), 387-401.

Vidic T., Fajfar P. and Fischinger M. [1994] "Consistent inelastic design spectra: strength and displacement", Earthquake Engineering and Structural Dynamics, 23, 502-521.

Zerbin, M., Aprile, A. [2015] "Sustainable retrofit design of RC frames evaluated for different seismic demand", Earthquakes and Structures, 9(6), 1337-1353.

Appendix A

The chord rotation at yielding, $\theta_{y,j}$, and at ultimate, $\theta_{um,j}$, the flexural, $V_{y,j}$, and shear strength, $V_{R,j}$, of the existing columns, beams and walls were estimated according to EC8-Part III [2005] and the Greek Code for interventions [GRECO, 2014]. The following expressions were used:

For beams or rectangular columns:

$$\theta_{y,i} = (1/r)_y \frac{L_s + a_v z}{3} + 0.0014\left(1 + 1.5\frac{h}{L_s}\right) + \frac{(1/r)_y d_b f_y}{8\sqrt{f_c}} \quad \text{(A1a)}$$

For walls:

$$\theta_{y,i} = (1/r)_y \frac{L_s + a_v z}{3} + 0.0013 + \frac{(1/r)_y d_b f_y}{8\sqrt{f_c}} \quad \text{(A1b)}$$

For beams or rectangular columns:

$$\theta_{um,j} = 0.016(0.3^{\nu})\left[\frac{\max(0.01, \omega')}{\max(0.01, \omega)} f_c\right]^{0.225} (a_s)^{0.35} 25^{\left(a\rho_s \frac{f_{sw}}{f_c}\right)} (1.25^{100\rho_d}) \quad \text{(A2)}$$

where a_v=1 if the shear force at flexural yielding, M_y/L_s, exceeds the shear at diagonal cracking, or 0 otherwise, z is internal lever arm equal to 0.9d in beams or columns, $0.8l_w$ in walls, d_b: diameter of longitudinal bars, a_w=1 for walls, 0 otherwise; ρ_s: confining reinforcement ratio in the direction of bending; ρ_d is diagonal reinforcement ratio. Material strengths f_y, f_c are in MPa. In members not detailed for earthquake resistance, the right hand of Eq. (A2) is reduced by 20%.

For every vertical member the flexural strength, $V_{y,j}$, was estimated by considering EC8-Part III [2005] and the Greek Code for interventions [GRECO, 2014] expressions according to which flexural capacities are converted into associated shear forces, $V_{y,j}=M_{y,j}/L_s$. This may be done assuming attainment of flexural capacity at both ends for the columns (shear span L_s equal to half the clear storey height), or a shear span

L_s of walls equal to 2/3 of the total height of the building. The yield moment, M_y, may be computed according to Eq. (A3).

$$\frac{M_{y,i}}{bd^3} = (1/r)_{y,i}\left\{E_c\frac{\xi_{y,i}^2}{2}\left(0.5(1+\delta)-\frac{\xi_{y,i}}{3}\right)+\left[\left(1-\xi_{y,i}\right)\rho+\left(\xi_{y,i}-\delta'\right)r'+\frac{\rho_v}{6}\left(1-\delta'\right)\right]\left(1-\delta'\right)\frac{E_s}{2}\right\} \quad (A.3)$$

The shear resistance of beams, columns and walls, $V_{R,\,i}$, with rectangular web (with units: MN and meters) was calculated according to

$$V_{R,i} = \frac{h-x}{2L_s}\min\left(N;0.55A_{c,i}f_c\right)+\left(1-0.05\min\left(5,\mu_{\theta,i}^{pl}\right)\right)\left[0.16\max\left(0.5;100\rho_{tot,i}\right)\left(1-0.16\min\left(5;a_s\right)\right)\sqrt{f_c}A_{c,i}+V_{w,i}\right] \quad (A4a)$$

The shear strength of a concrete wall, $V_{R,\,j}$, may not be taken greater than the value corresponding to failure by web crushing, $V_{R,\,max,\,j}$, which under cyclic loading may be calculated from the following expression (with units: MN and meters):

$$V_{R,\max,i} = 0.85\left(1-0.06\min\left(5;\mu_{\theta,i}^{pl}\right)\right)\left(1+1.8\min\left(0.15;\frac{N_i}{A_{c,i}f_c}\right)\right)\left(1+0.25\max\left(1.75;100\rho_{tot,i}\right)\right)\left(1-0.2\min\left(2;a_s\right)\right)\sqrt{f_c}b_{w,i}z_i \quad (A4b)$$

where $\mu_{\theta,i}^{pl}$ is the ratio the plastic part of the chord rotation, θ, normalized to the chord rotation at yielding, θ_y. In the calculations, $\mu_{\theta,i}^{pl}$ was assumed equal to 0.

Appendix B

TABLE B1 Dimensions and reinforcing details of R.C. jacketed members.

R.C. Jacketed Columns							
Column	b_x (mm)	b_y (mm)	Long. Reinforcement (mm)	Stirrups (mm)	ρ_{itot} (%)	ΔK_x (kN/m)	ΔK_y (kN/m)
1st Storey							
C6	500	500	8Ø20	Ø10/120	0.91%	1854.6	2408.9
C7	400	450	8Ø20	Ø10/120	1.40%	1617.2	2075.3
C8	500	550	8Ø20	Ø10/120	0.91%	2317.6	2611.6
C10	450	500	8Ø20	Ø10/120	1.12%	1886.5	2394.3
C12	550	550	8Ø20	Ø10/120	0.83%	2435.8	2435.8
C13	400	400	8Ø22	Ø10/120	1.90%	2032.3	2032.3
C14	450	450	8Ø20	Ø10/120	1.24%	1844.3	2024.3
C17	550	500	8Ø20	Ø10/120	0.91%	2607.1	2314.9
C18	400	400	8Ø22	Ø10/120	1.90%	1878.1	1976.8
C21	400	450	8Ø20	Ø10/120	1.40%	1567.3	2026.2
C22	500	500	8Ø20	Ø10/120	1.01%	2340.9	2340.9
C23	400	400	8Ø20	Ø10/120	1.57%	1590.2	1590.2
C26	450	450	8Ø20	Ø10/120	1.24%	1775.5	1775.5
C27	450	400	8Ø20	Ø10/120	1.40%	1652.3	1421.2
C28	500	450	8Ø20	Ø10/120	1.12%	2310.4	1803.5
2nd Storey							
C12	450	550	8Ø20	Ø10/120	1.02%	4978.7	7362.2
C14	400	450	8Ø18	Ø10/120	1.13%	3507.4	4523.3
C17	425	400	8Ø20	Ø10/120	1.48%	4231.4	3753.1
C18	450	400	8Ø20	Ø10/120	1.40%	5450.5	4642.2
C28	450	450	8Ø20	Ø10/120	1.24%	5175.2	5291.8